

## Article

# Preparation of Magnesium Ammonium Phosphate Mortar by Manufactured Limestone Sand Using Compound Defoaming Agents for Improved Strength and Impermeability

Wenting Mao <sup>1,\*</sup> , Chunpeng Cao <sup>1</sup>, Xincheng Li <sup>1</sup>, Jueshi Qian <sup>2</sup> and Chao You <sup>3</sup>

<sup>1</sup> Yunnan Academy of Building Research Co., Ltd., Kunming 650223, China; caochpeng@163.com (C.C.); xinchengli@aliyun.com (X.L.)

<sup>2</sup> College of Materials Science and Engineering, Chongqing University, Chongqing 400044, China; qianjueshi@126.com

<sup>3</sup> Guizhou Magnesium Phosphate Materials Co., Ltd., Guiyang 550002, China; chaoyoulm@126.com

\* Correspondence: wm280@alumni.cam.ac.uk; Tel.: +86-180-8795-1969

**Abstract:** Magnesium ammonium phosphate cement (MAPC) mortar has recently risen up as high performance rapid repair material for concrete structures. But high costs of the raw materials limit its restoration and maintenance projects on a wide application range. This study proposes the use of manufactured limestone sand with lower cost and wider range of sources in replacement of quartz sand as fine aggregates to produce MAPC mortar. However, the limestone fines of manufactured sand were initially found to have negative effects on the performance of MAPC mortar, causing significant blistering and volume expansion and decreased compressive strength and interfacial bonding strength. To minimize these negative effects, polyether modified silicone (PMS) defoamer and its compound use with mineral admixtures Portland cement and silica fume were investigated on the effectiveness in reducing expansion and improving other properties of MAPC mortar. Results showed that the compound use of PMS defoamer and Portland cement as a new defoaming formula effectively reduced the volume expansion from 7.92% to 0.91%. The compressive strength and interfacial bonding strength were significantly improved by over 34% and 60% respectively. Moreover, this defoaming formula showed improvements in water-tight performance and resistance to chloride penetration. According to the mercury intrusion porosimetry (MIP) analysis, the total porosity of MAPC mortar after defoaming treatment was decreased by about 40% and the pore structure was also modified to be finer by significantly reducing the harmful macropores. Overall, the use of manufactured limestone sands as fine aggregates turned out to be a feasible and economic approach for promoting the field application of MAPC mortar.

**Keywords:** magnesium ammonium phosphate mortar; manufactured limestone sand; expansion; compound defoaming admixture; mechanical strength; impermeability



**Citation:** Mao, W.; Cao, C.; Li, X.; Qian, J.; You, C. Preparation of Magnesium Ammonium Phosphate Mortar by Manufactured Limestone Sand Using Compound Defoaming Agents for Improved Strength and Impermeability. *Buildings* **2022**, *12*, 267. <https://doi.org/10.3390/buildings12030267>

Academic Editors: Shengwen Tang and Lei Wang

Received: 26 January 2022

Accepted: 17 February 2022

Published: 24 February 2022

**Publisher's Note:** MDPI stays neutral with regard to jurisdictional claims in published maps and institutional affiliations.



**Copyright:** © 2022 by the authors. Licensee MDPI, Basel, Switzerland. This article is an open access article distributed under the terms and conditions of the Creative Commons Attribution (CC BY) license (<https://creativecommons.org/licenses/by/4.0/>).

## 1. Introduction

Following the global construction boom, the maintenance technology of concrete structures has come into focus in the area of civil engineering. Concrete structures in service have been experiencing performance degradation due to various interior or exterior actions such as sustained loading and environmental corrosions. Magnesium phosphate cement (MPC) has recently raised attention as rapid repair material for concrete structures [1,2]. MPC has the properties of chemically bonded ceramics and is quite different from ordinary Portland Cement (OPC) in terms of raw material characteristics, hydration process, and hydrate composition [3]. It is a new type of cementitious material with chemical bonding formed by through-solution mechanism and acid-based reaction between phosphate and dead burnt magnesia [4,5]. Among various rapid repair cementitious materials, MPC outstands for the extremely quick hardening, high early strength, and good bonding to

old concrete substrate [2,4,6–8] which meet the requirements of rapid repair for projects on highways, municipal roads, airfield pavements, and building structures. It also has some unique properties such as excellent strength development under subzero temperature environment, minor shrinkage, and good abrasion resistance [2,9]. Such unique properties allow the use of MPC materials in some projects under extreme service environment.

Magnesium ammonium phosphate cement (MAPC) is one of the typical types of MPC system materials. MAPC is prepared by dead burned magnesia (MgO), ammonium dihydrogen phosphate ( $\text{NH}_4\text{H}_2\text{PO}_4$ ), and retarder such as borax [2,10]. ADP reacts rapidly with MgO to produce stable hydration products  $\text{NH}_4\text{MgPO}_4 \cdot 6\text{H}_2\text{O}$  (struvite) which constructs the high strength structure of MAPC. The chemical reaction is as Equation (1) [2].



The setting time of MAPC can be flexibly regulated from minutes to tens of minutes and the early compressive strength at 1 h can reach up to 30 MPa or even higher [11]. The bonding strength at 3 days could reach above 3 MPa [12]. The reaction process of MAPC is accompanied by intense heat release. MAPC is therefore usually mixed with aggregates into mortar admixtures or concrete to avoid overheating and obtain an optimal strength in practical application [2]. To ensure the high performance of MAPC mortar, quartz sands is commonly used as fine aggregates due to its high cleanness and well gradation [2,13,14]. However, MAPC itself is expansive in terms of the raw materials and costs several or even a dozen times conventional cementitious materials. The incorporation of expansive quartz sand further increases the cost of MAPC mortar. River sand was also tested as fine aggregates for producing MAPC mortar which showed slightly lower strength than the mortar formulated with quartz sand [3]. Nonetheless, natural river sand resources are confronted with the situation of exhausting and the exploitation has been forbidden due to environmental destruction and pollution [15,16]. In construction practice, manufactured limestone sand is extensively used as fine aggregates due to its low cost and wide availability. The use of manufactured limestone sand as an alternative for quartz sand is considered more economic and advantageous in the promotion and application of MAPC mortar.

In normal Portland cement concrete system, the properties of manufactured limestone sand have been widely investigated [17,18], especially the effects of limestone fines content on performance of concrete materials. But in MAPC mortar system, the rational use and possible effects of manufactured limestone sand was rarely reported. This study explores the feasibility of preparing high performance MAPC mortar using manufactured limestone sand. The trial preparation of MAPC mortar by manufactured sand containing different contents of limestone fines was first carried out in this study. The volume stability and mechanical strength of MAPC mortar were tested. In view of the excessive blistering and expansion problems caused by limestone fines in MAPC mortar, possible solutions to inhibiting blistering was explored. An effective compound defoaming agent was eventually proposed to reduce expansion and improve the mechanical strength and impermeability performance.

## 2. Material and Methods

### 2.1. Material

#### 2.1.1. Magnesium Ammonium Phosphate Cement (MAPC)

Dead burned MgO was produced by calcination of magnesite ( $\text{MgCO}_3$ ) over 1700 °C, with an average particle size (D50) of 10.4 µm and a purity of 97%. Ammonium dihydrogen phosphate (ADP) from Guizhou Magnesium Phosphate Materials Co., Ltd., Guizhou, China is industrial grade with an average particle size (D50) of 3.04 µm and a purity over 98%. Borax ( $\text{Na}_2\text{B}_4\text{O}_7 \cdot 10\text{H}_2\text{O}$ ) with a purity over 99% is used as retarder.

MAPC is prepared by admixtures of MgO, ADP, and retarder. The P/M (ADP to MgO) ratio is 3/8 and the dosage of retarder is 4% of the sum of ADP and MgO.

### 2.1.2. Fine Aggregates

The limestone manufactured sand was obtained from a local quarry in Yuxi, Yunnan province. The maximum particle size is 2.36 mm. Three groups of the limestone sand with different contents of limestone fines ( $\leq 0.075$  mm) at 0%, 10%, and 20% were prepared. The chemical contents of limestone fines mainly consist of  $\text{CaCO}_3$  (89.93%), and also small fractions of  $\text{MgO}$ ,  $\text{SiO}_2$ ,  $\text{Al}_2\text{O}_3$ ,  $\text{Fe}_2\text{O}_3$ . The average particle size (D50) of limestone fines is 11.4  $\mu\text{m}$ . The quartz sand used is ISO standard sand with maximum particle size of 2.36 mm, obtained from China ISO Sand Co., Ltd., Xiamen, China.

### 2.1.3. Defoaming Admixtures

Polyether modified silicone (PMS) defoamer PXP-3 is obtained from Sobute New Materials Co., Ltd., Nanjing, China. In this study, mineral admixtures including silica fume and Portland cement are also tested as defoaming agents. The silica fume obtained from SLT Co., Ltd., Chengdu, China has an average particle size of 0.26  $\mu\text{m}$ . Portland cement used in this study is Reference Cement from China United Cement Co., Ltd., Shandong, China.

## 2.2. Preparation Methods of MAPC Mortar

The MAPC mortar was prepared with MAPC and fine aggregates (limestone sand or quartz sand) at a mix ratio of 1:1. The water to binder ratio ( $m_{\text{water}}/m_{\text{MAPC}}$ ) was 0.17. Three groups of the limestone sand with limestone fines at dosage of 0%, 10%, and 20% were used for preparation of MAPC mortar. One reference group of MAPC mortar with quartz sand was also prepared. The MAPC powders and sands were first dry mixed for 60 s at low speed in the planetary mixer. After water addition, the paste was wet mixed at low speed for 30 s and then another 90 s at high speed. The properties of each fresh mortar (fluidity, setting time, volume stability) were tested immediately after mixing. The mortar was also cast in different molds and demolded after 30 min, then continued to be cured under lab environment (20 °C, 50% RH) for further tests on mechanical strength and impermeability performance.

For the addition of defoaming agents, the liquid PMS defoamer was first dispersed in mixing water and then added in the mortar mixtures while powdery silica fume or reference cement was added during dry mixing before water addition.

## 2.3. Properties of MAPC Mortar with Limestone Sand

### 2.3.1. Flowability and Setting Time

The fluidity of MAPC mortar was tested by flow cone method according to ASTM C939-10 standard [19]. The setting time was determined by the modified Vicat needle apparatus in accordance with ASTM C187 standard [20]. Due to the initial setting time is very close to the final setting time in MAPC mortar, the initial setting time was usually used to characterize its setting and hardening behavior.

### 2.3.2. Volume Stability

The volume stability of MAPC mortar was characterized by the linear deformation rate during early age before setting and later age after setting. The linear deformation of MAPC mortar in fluid state before setting was measured using a graduated cylinder apparatus according to JTG 3420-2020 (T 0518-2020) [21], as shown in Figure 1. The mortar was cast into the cylinder immediately after mixing and the readings of level height were recorded every 30 s until 30 min after mixing. For the volume change after hardening, prisms (25 mm  $\times$  25 mm  $\times$  280 mm) were tested for the linear deformation using a digital length comparator following the instruction of ASTM C596-18 [22]. The initial measurement was conducted immediately after demolding and continued in the following 112 days.

Three replicate specimens were used for measurements of each mix group. The linear deformation rate  $\Delta R$  was calculated as in Equation (2).

$$\Delta R = 100\% \times (L_1 - L_0) / L_0 \quad (2)$$

where  $L_0$  is the initial level height of fresh mortar or the initial length of prism;  $L_1$  is the level height of fresh mortar or the length of prism at each curing age.

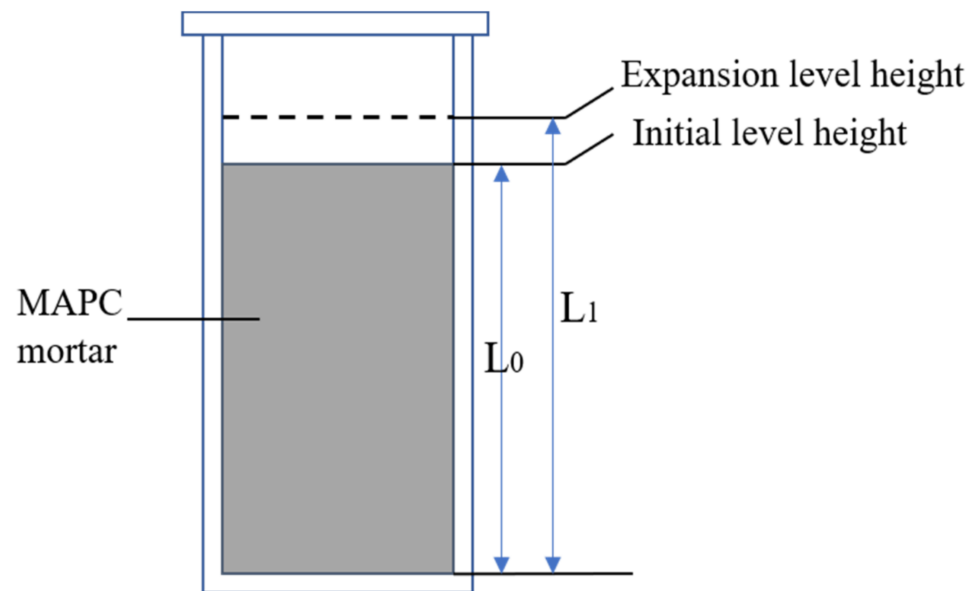


**Figure 1.** Testing apparatus of linear expansion of fresh MAPC mortar before setting.

### 2.3.3. Compressive Strength

The MAPC mortar samples were tested for compressive strength respectively at 1 h, 3 h, 3 days, 28 days according to ISO 679 standard [23]. The cubic specimens (40 mm × 40 mm × 40 mm) were tested for the unconfined compressive strength (UCS) using a 300 kN microcomputer-controlled electronic pressure testing machine at a loading rate of 2400 N/s. Each group of specimens were tested in triplicate and the average value was taken.

### 2.3.4. Interfacial Bonding Strength

As repair material, MAPC mortar samples were tested for interfacial bonding strength with ordinary concrete matrix. The test method was modified from splitting tensile strength test in GB/T 50081-2002 [24]. A split cylinder mold (Figure 2) consisting of two half cylinders was designed for sample casting. The ordinary concrete matrix with designated strength grade of C50 was first cast in one half cylinder and cured for 28 days. Then the MAPC mortar was cast in the other half cylinder bonded with the ordinary concrete, which formed a complete cylinder. After curing for 3 days and 28 days, the complete cylinder was tested for splitting tensile strength using a 3000 kN electronic universal testing machine at a loading rate of 0.08 MPa/s. The interfacial bonding strength of MAPC mortar with ordinary concrete matrix was evaluated by the splitting tensile strength of the complete cylinder. Each group of specimens were tested in quadruplicate and the average value was taken.

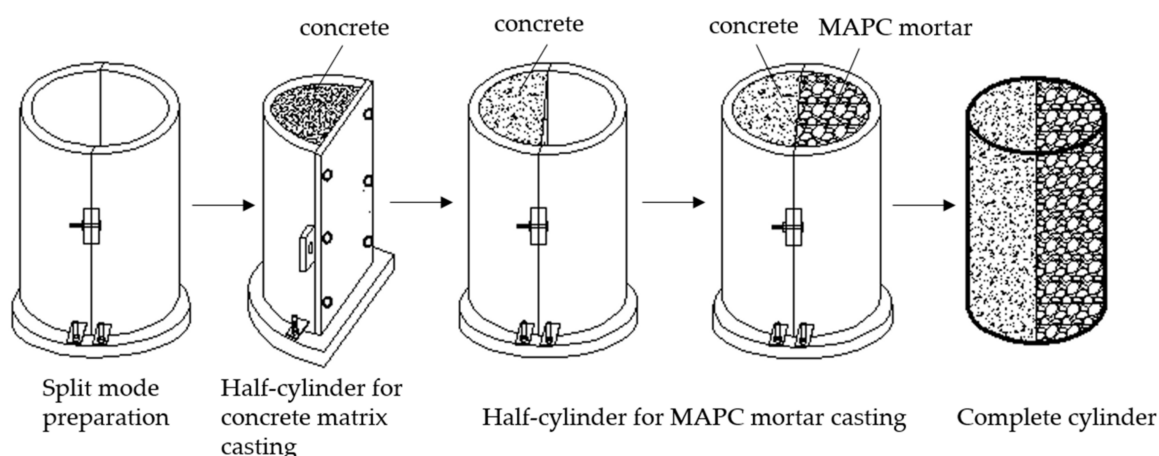


**Figure 2.** Sample preparation for test on interfacial bonding strength of MAPC mortar with ordinary concrete matrix.

### 2.3.5. Water-Tight Performance

After curing for 28 days, the MAPC mortar samples in the shape of frustum of a cone (top diameter 70 mm; bottom diameter 80 mm; height 30 mm) were tested for water-tight performance according to JGJ/T 70-2009 standard [25]. A mortar impermeability apparatus (HP-4.0) was used to apply hydraulic pressure on the specimens at a pressurizing rate of 0.1 MPa/h. Six samples were prepared for each test group. When 3 out of 6 specimens failed under hydraulic pressure, the test was terminated and the correspondent pressure value was recorded. The impermeability pressure was defined as Equation (3).

$$P = H - 0.1 \quad (3)$$

where  $P$  is the impermeability pressure, MPa;  $H$  is the pressure when 3 out of 6 specimens failed, MPa.

### 2.3.6. Resistance to Chloride Ion Penetration

After curing for 28 days, the cylindrical MAPC mortar specimens ( $\Phi$  100 mm; 50 mm thick) were tested for resistance to chloride ion penetration according to ASTM C1202 standard [26]. During a 6-h period, a potential difference of 60 V dc is maintained across the ends of the specimen, one of which is immersed in a sodium chloride solution, the other in a sodium hydroxide solution. The total charge passed, in coulombs (C), is used to evaluate the resistance of the specimen to chloride ion penetration.

### 2.3.7. Microstructure Analysis

For mercury intrusion porosimetry (MIP), cubic fragments in size of 1 cm  $\times$  1 cm  $\times$  1 cm were prepared at the curing age of 28 days. The fragments were treated with absolute ethyl alcohol for terminating hydration and then dried in the oven at 40 °C. The fragments after treatment were stored in the vacuum chamber until testing.

## 3. Results and Discussion

### 3.1. Effects of Limestone Fines on MAPC Mortar

#### 3.1.1. Volume Stability

Compared with reference group with quartz sand, MAPC mortar prepared by manufactured sand with limestone fines (10% and 20%) were observed to generate a lot of air bubbles, accompanied by significant volume expansion before hardening. Meanwhile, the sample prepared by manufactured sand without limestone fines (0%) showed only slight expansion similar to the reference group. Obviously, it is the limestone fines that caused severe volume expansion of MAPC mortar. As shown in Figure 3, the volume expansion

before hardening induced by limestone fines reached up to 7.92% within 10 min, while the reference samples without limestone fines only showed slight expansion less than 0.8%. Furthermore, the long-term volume stability tests were also carried out. After hardening, MAPC mortar with limestone fines showed good volume stability just as the reference samples, with a very low degree of shrinkage less than 0.01%. The limestone fines seemed to affect only the volume changes before hardening.

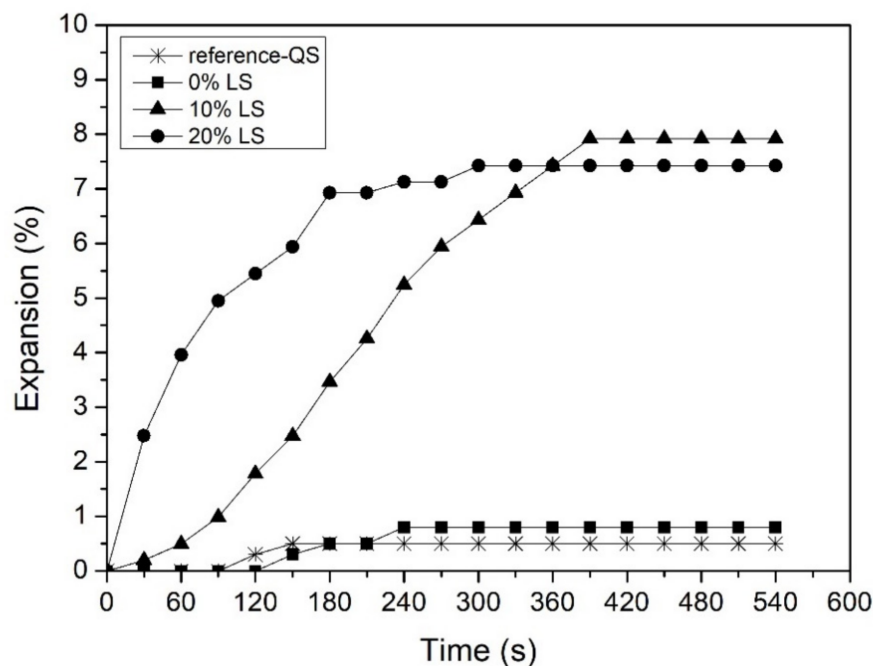


**Figure 3.** Expansion (before setting) of MAPC mortar samples with limestone fines (LS) at different dosage of 0%, 10%, 20% (by weight of MAPC).

The limestone fines mainly consist of calcium carbonates ( $\text{CaCO}_3$ ) which tend to rapidly react with ADP during mixing.  $\text{CaCO}_3$  can be more reactive than dead burned  $\text{MgO}$  in reaction with the phosphate to form calcium phosphate hydrates [27,28]. The pH value of limestone fines in water solution was tested as 9.51 which was higher than that of  $\text{MgO}$  as 7.89. Apparently, limestone powder with high alkalinity is more likely to first react with acidic ADP. It is known that the chemical reaction of MAPC is accompanied by  $\text{NH}_3$  gas generation [2,6], which induced slight expansion as shown in reference sample. However, the reaction between  $\text{CaCO}_3$  and ADP could further generate  $\text{CO}_2$  apart from  $\text{NH}_3$ . As a result, the formation of air bubbles intensified and thus blew up the fresh MAPC mortar, causing severe expansion.

### 3.1.2. Mechanical Strength

Without limestone fines, MAPC mortar prepared with limestone sand showed compressive strength of 31.08 MPa at 1 h and 71.12 MPa at 28 days which was comparable to that of reference sample with quartz sand. The compressive strength at 3 days of sample with 0% limestone fines was even higher than that of the reference sample. It is inferred that the rough surface of limestone sand provided stronger mechanical interlocking with MAPC binder which enhanced the mechanical properties. However, MAPC mortar samples with 10% and 20% limestone fines experienced compressive strength degradation at early age and this trend exacerbated at later age, as shown in Figure 4. For the group with 10% limestone fines, the compressive strength decreased by 15.23% at 1 h and 25.07% at 28 days respectively. As the limestone fines content increased to 20%, the compressive strength further decreased by 17.12% at 1 h and 31.86% at 28 days respectively. It is inferred that ex-

cessive blistering and expansion before hardening led to increased porosity and formation of harmful pores in the hardened mortar matrix and then decrease in compressive strength.

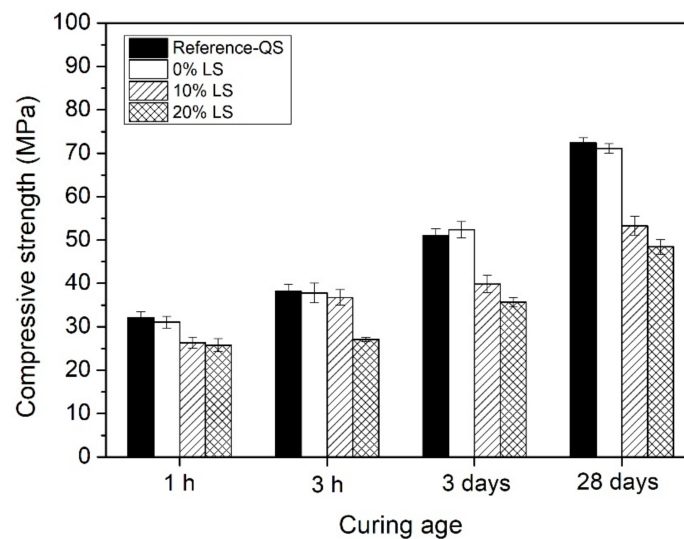


**Figure 4.** Compressive strength at different curing ages of 1 h, 3 h, 3 days, 28 days of MAPC mortar samples with quartz sand (Reference-QS) and limestone fines (LS) at different content of 0%, 10%, 20%.

In the meantime, limestone fines were found to have negative influence on the interfacial bonding strength of MAPC mortar with ordinary concrete matrix. In Figure 5, the interfacial bonding strength of reference sample reached 2.99 MPa and 4.28 MPa at 3 days and 28 days respectively. As the content of limestone fines increased from 0% to 10%, the interfacial bonding strength of MAPC mortar dramatically decreased by more than 60% at both early and later age. With content of 20% limestone fines, the interfacial bonding strength of MAPC mortar dropped to 0.92 MPa and 1.25 MPa at 3 days and 28 days respectively. After loading, a large number of pores were observed on the broken interface of half MAPC matrix. Because of the blistering caused by limestone fines, air bubbles were prone to agglomerate at the bonding interface which reduced the effective bonding area between MAPC mortar and ordinary concrete matrix. Moreover, the mechanical strength of MAPC mortar itself decreased with increasing limestone fines as aforementioned. As a result, the interfacial bonding strength was significantly reduced.

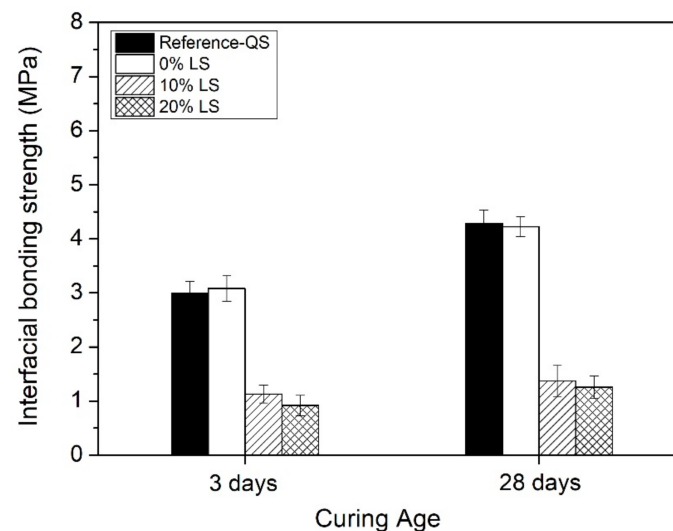


**Figure 5.** Interfacial bonding strength at different curing ages of 3 days, 28 days of MAPC mortar samples with quartz sand (Reference-QS) and limestone fines (LS) at different contents of 0%, 10%, 20%.

As a whole, limestone fines can cause volume expansion in MAPC mortar and consequent strength decrease. Apparently, how to solve the bubbling problem caused by limestone fines is the key to effective utilization of manufactured limestone sand resources. One common solution is water processing to remove limestone fines from manufactured sands. But this treatment brings about severe water consumption and waste, and also environmental pollutions. An effective and economical solution is needed for tackling the adverse effects of limestone fines in MAPC materials.

### 3.2. Efficacy of Different Admixtures on Expansion Reduction

Ideally, the MAPC mortar with limestone fines is expected to remain as low expansion as the reference sample without limestone fines. To achieve this goal, different types of admixtures, including polyether modified silicone (PMS) defoamer, silica fume, and reference cement, were tested for performance on defoaming and expansion reduction in MAPC mortar system with 10% limestone fines.

#### 3.2.1. Polyether Modified Silicone (PMS) Defoamer

Polyether-modified silicone (PMS) defoamer were added at a dosage of 0.15%, 0.3%, 0.6%, and 1% (by weight of MAPC) respectively in MAPC mortar during mixing. The results on expansion reduction performance are shown in Figure 6. Compared with reference samples, the addition of PMS defoamer shows certain effectiveness in reducing the bubbling effect. With 0.15% PMS defoamer, the expansion of MAPC mortar before hardening was reduced from 7.92% to 5.00%. The expansion could be further reduced to 3.94% (almost 50% reduction) as the dosage of PMS defoamer increased to 0.3%. The PMS defoamer can quickly reduce the surface tension on liquid membrane and decrease the foam stability, thereby breaking foam and restraining foam formation. However, overdose addition would weaken the defoaming effect [29]. At higher content of 0.6% and 1%, PMS defoamer could only reduce the expansion from 7.92% to 4.48% and 6.0% respectively. This can be due to decreased fluidity of MAPC mortar caused by overdose of PMS defoamer. It was observed that the MAPC mortar became much more viscous as the PMS defoamer were added over 0.3%. The PMS defoamer is basically a liquid organic agent with hydrophobic nature. Its emulsion in mixing water could affect dissolution of ADP and fully mixing of all the contents, therefore decreasing the fluidity. The decreased fluidity could further lead to suppression of bubble overflow and also insufficient dispersion of PMS defoamer in fresh MAPC mortar.

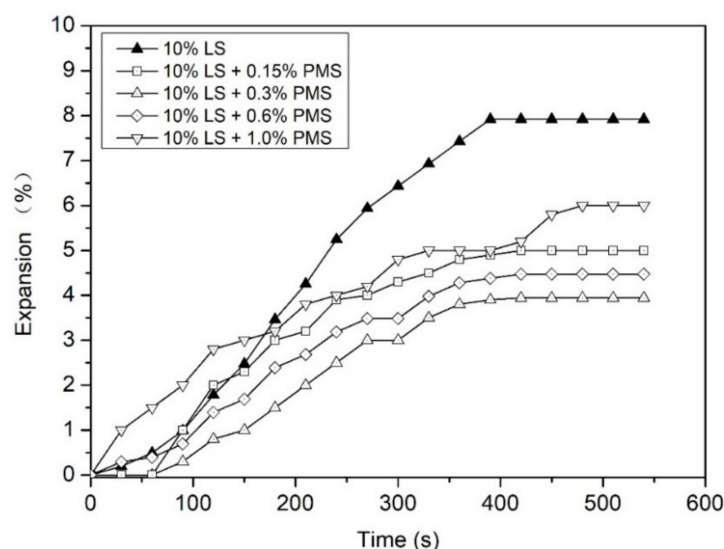


**Figure 6.** Expansion (before setting) of MAPC mortar samples with 10% limestone fines (LS) with or without defoaming treatment by polyether modified silicone (PMS) defoamer at different dosage of 0.15%, 0.3%, 0.6%, and 1% (by weight of MAPC).

In conclusion, the PMS defoamer has a certain effect on breaking bubbles caused by limestone fines in MAPC mortar and the proper dosage is 0.3%. But its defoaming efficacy is still insufficient for completely eliminating the bubbles and the consequent expansion.

### 3.2.2. Compound Defoaming Admixtures

Given that the organic PMS defoamer works on the physical principles of defoaming, mineral admixtures were considered for tests on inhibiting the bubbles generation based on the chemical reaction principles. On the basis of PMS defoamer, the hybrid use of mineral admixtures is expected to enhance the defoaming efficacy in MAPC mortar by combining both physical and chemical approaches. Silicon/aluminum mineral admixtures such as silica fume, metakaolin, and Portland cement have been reported to be used in improving the physico mechanical properties of magnesium potassium phosphate cement (MKPC) by intervening in the reactions between MKPC components [30–33], which offers a reference for use in the MAPC system in this paper.

Portland cement (reference cement) and silica fume were chosen for investigation in this paper due to their accessibility in the local area. In MAPC mortar system with 10% limestone fines, the mineral admixture was added at 1% and 3% (by weight of MAPC) respectively in MAPC mortar for testing the performance on defoaming and expansion reduction. In the meantime, the PMS defoamer was added at a constant dosage of 0.3% (by weight of MAPC).

In Figure 7a, with the compound use of PMS defoamer, Portland cement was surprisingly found to have positive effect on further inhibiting bubbles and reducing expansion. The expansion of MAPC mortar with 1% Portland cement and 0.3% PMS defoamer showed only 0.91% which was very close to the same level of the reference mortar samples at 0.59%. As the dosage of Portland cement increased to 3%, the expansion eventually leveled at 0.5%, which was even lower than the reference sample. However, it was noted that increasing dosage of Portland cement could shorten the setting time of MAPC mortar. The setting time of reference sample with quartz sand and 0% limestone fines was 17–19 min. The addition of 3% Portland cement obviously shortened the setting time to 7 min and the expansion also quickly leveled down. Such short setting time usually cannot meet the demands of construction time on sites. By contrast, the samples with 1% Portland cement still remained a setting time of 16 min similar to that of the reference sample.

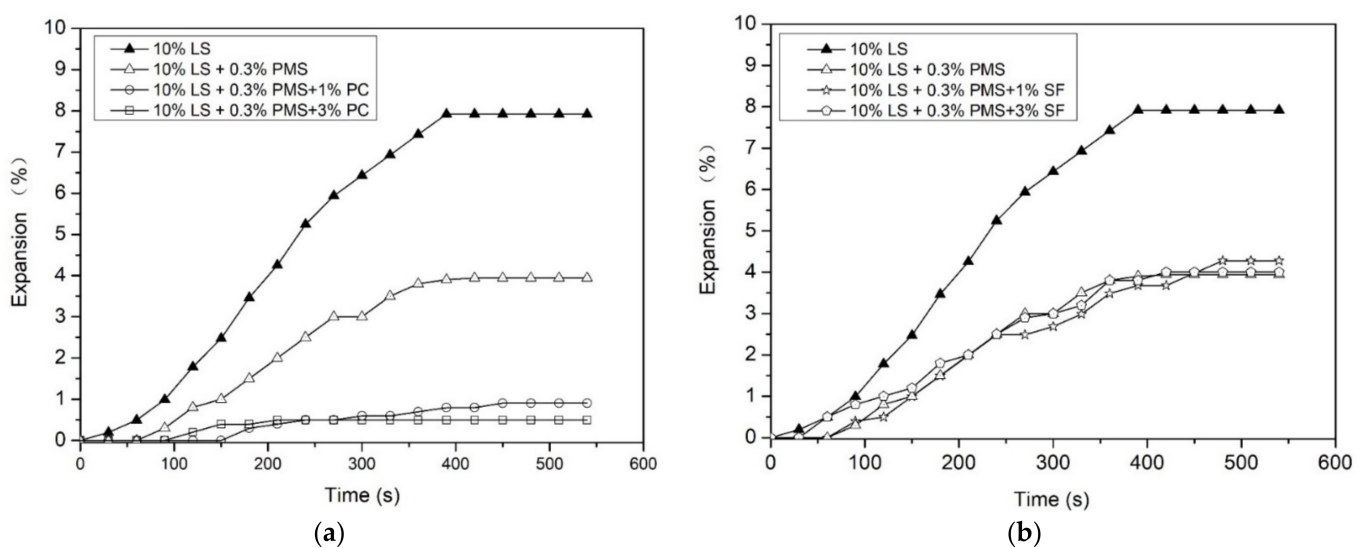


**Figure 7.** Expansion (before setting) of MAPC mortar samples with 10% limestone fines (LS) with or without defoaming treatment by the compound use of 0.3% polyether-modified silicone (PMS) defoamer and (a) Portland cement (PC); (b) silica fume (SF) at dosage of 1% and 3% (by weight of MAPC).

When mixed with MAPC, the main contents of Portland cement ( $C_2S$ ,  $C_3S$ ,  $C_3A$ ,  $C_4AF$ ) and its hydration product  $Ca(OH)_2$  could react with ammonium dihydrogen phosphate (ADP) to form phosphate calcium compounds as binding materials similar to struvite [31,34]. Especially,  $C_3A$  which hydrates the fastest is supposed to first react with ADP during mixing. Furthermore, the solution around Portland cement particles tends to be of strong alkalinity, which promotes the reaction with acidic ADP. By contrast,  $CaCO_3$  with poor water-solubility shows weak alkalinity in water solution. In this paper, tests showed that pH value of Portland cement and  $CaCO_3$  in water solution was 12.27 and 9.51 respectively. In the system of MAPC mortar containing limestone fines, Portland cement with higher alkalinity and active constituents was more likely to react faster with ADP than  $CaCO_3$ , thereby inhibiting the reaction of  $CaCO_3$  and  $CO_2$  bubbles generation. As mentioned above, only 1% Portland cement was needed to achieve defoaming effect. Overuse would cause accelerated hardening.

As in Figure 7b, MAPC mortar with the extra addition of silica fume at 1% and 3% showed expansion of 4.28% and 4.0% respectively. In contrast with individual addition of PMS defoamer, silica fume did not show obvious effect on enhancing the defoaming process. Moreover, the increasing dosage of silica fume was found to reduce the fluidity of MAPC mortar. As for silica fume, the pH value is 7.6 which is close to neutral. Its main content  $SiO_2$  can only be activated in alkaline environment [35]. But the interior environment of MAPC mortar is acidic at early age due to the fast dissolution of ADP. Under such environment, neutral silica fume could not effectively react with ADP and inhibit bubbling caused by  $CaCO_3$ . The silica fume particles mainly play a role of micro-filling instead of active reactant in MAPC mortar. With addition of silica fume, its micro-filling effect, high specific surface area and water demand lead to decreased fluidity of MAPC mortar. As a result, the mortar mixture became more viscous which was unfavorable for the overflow of bubbles.

In conclusion, the formula of 0.3% PMS defoamer and 1% Portland cement was proved to be effective compound defoaming admixtures for MAPC mortar containing limestone fines. Moreover, this formula was also tested for expansion reduction in MAPC mortar system with 20% limestone fines and only small degree of expansion of 0.80% was observed. It suggests that this formula should be effective within a range of 0–20% limestone fines.

### 3.3. Improvement on Mechanical Properties of MAPC Mortar after Defoaming

After treated with compound defoaming admixture (0.3% PMS defoamer and 1% Portland cement), MAPC mortar samples with 10% and 20% limestone fines were tested for compressive strength and interfacial bonding strength at different curing ages. The test results suggest significant improvements on both compressive strength and interfacial bonding strength of MAPC mortar samples after defoaming treatment. In Figure 8, for samples with 10% limestone fines, the compressive strength at 1 h and 28 days was improved by 40.83% and 34.83% respectively; for samples with 20% limestone fines, the compressive strength at 1 h and 28 days was improved by 35.17% and 40.59%. The compressive strength of MAPC mortar samples after defoaming treatment were almost comparable to that of reference samples. Effective defoaming treatment could decrease the porosity of MAPC mortar by reducing bubbles and refining large pores during reaction process before setting, thereby improving compressive strength. In Figure 9, over 60% increase in interfacial bonding strength of MAPC mortar samples with limestone fines was achieved after defoaming treatment, suggesting the effectiveness of defoaming compounds in inhibiting agglomeration of air bubbles at the bonding interface. The half MAPC mortar with denser structure and higher strength developed sufficient bonding area with the ordinary concrete matrix.

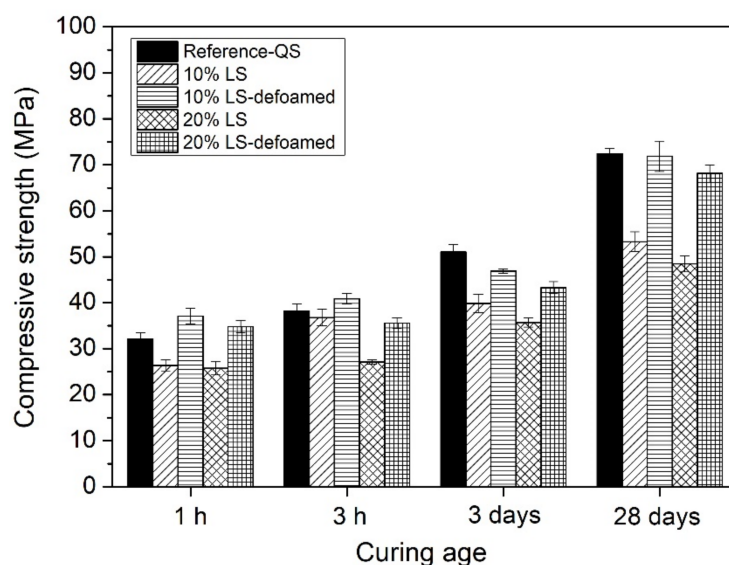


**Figure 8.** Compressive strength (at curing age of 1 h, 3 h, 3 days, 28 days) of MAPC mortar samples containing limestone fines (at content of 10% and 20%) with or without defoaming treatment by the compound use of 0.3% polyether modified silicone (PMS) defoamer and 1% Portland cement (PC).

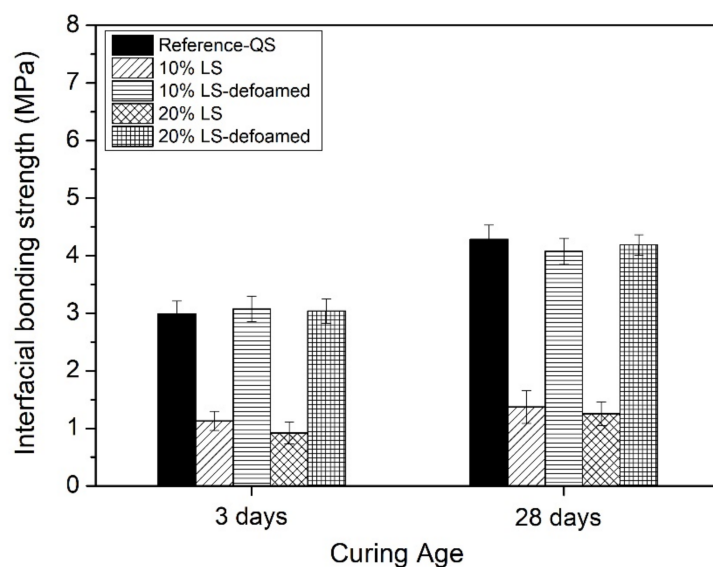


**Figure 9.** Interfacial bonding strength (at curing age of 3 days, 28 days) of MAPC mortar samples containing limestone fines (at content of 10% and 20%) with or without defoaming treatment by the compound use of 0.3% polyether modified silicone (PMS) defoamer and 1% Portland cement (PC).

### 3.4. Improvement on Impermeability of MAPC Mortar after Defoaming

The MAPC mortar samples with limestone fines after defoaming treatment also showed improvements on impermeability properties including resistance to chloride ion penetration and water-tight performance. As shown in Table 1, compared with reference samples with 10% limestone fines, the electric flux value of defoaming samples decreased from 2824 C to 869 C which suggested a high level of resistance to chloride ion penetration; the impermeability grade of defoaming samples was improved from 0.5 MPa to 0.9 MPa. Similarly, for samples with 20% limestone fines, the electric flux value of defoaming samples decreased from 3473 C to 733 C and the impermeability grade of defoaming samples was improved from 0.4 MPa to 0.7 MPa. The defoamed samples achieved even better impermeability performance compared with the reference sample. Obviously, the compactness of MAPC samples was improved after defoaming treatment. The densified pore

structure contributed to improved impermeability [36]. The pores, especially connected pores harmful to impermeability were effectively reduced by the compound defoaming admixtures. The modification of pore structures after defoaming would be discussed in the following part of microstructure analysis.

**Table 1.** Performance on resistance to chloride ion penetration and water-tightness of MAPC mortar with limestone fines (at content of 10% and 20%) or quartz sand (QS).

Group	Reference Sample with QS	MAPC with 10% Limestone Fines		MAPC with 20% Limestone Fines	
		Before defoaming	After defoaming	Before defoaming	After defoaming
Performance	/				
Electric flux value (C)	1015	2824	869	3473	733
Impermeability grade(MPa)	0.7	0.5	0.9	0.4	0.7

### 3.5. Microstructure Analysis

Mercury intrusion porosimetry (MIP) analysis on MAPC mortar samples were carried out to further investigate the modification on the pore structures induced by the compound defoaming admixtures. According to MIP results in Figure 10a, the reference samples with 10% limestone fines yielded a total intrusion volume of 10.83% and a total porosity of 21.65%; the reference samples with 20% limestone fines yielded a total intrusion volume of 12.98% and a total porosity of 24.72%. Higher content of limestone fines resulted in higher porosity of MAPC mortar. By contrast, the defoamed samples showed lower percentage of pore volume than the reference samples, with a total porosity of 13.17% and 14.78% respectively. The total porosity of both groups were decreased by around 40%. The defoamed samples were thus more compact and contains finer pore structure than the reference samples, apparently due to the effective defoaming effect of the compound defoaming admixtures.

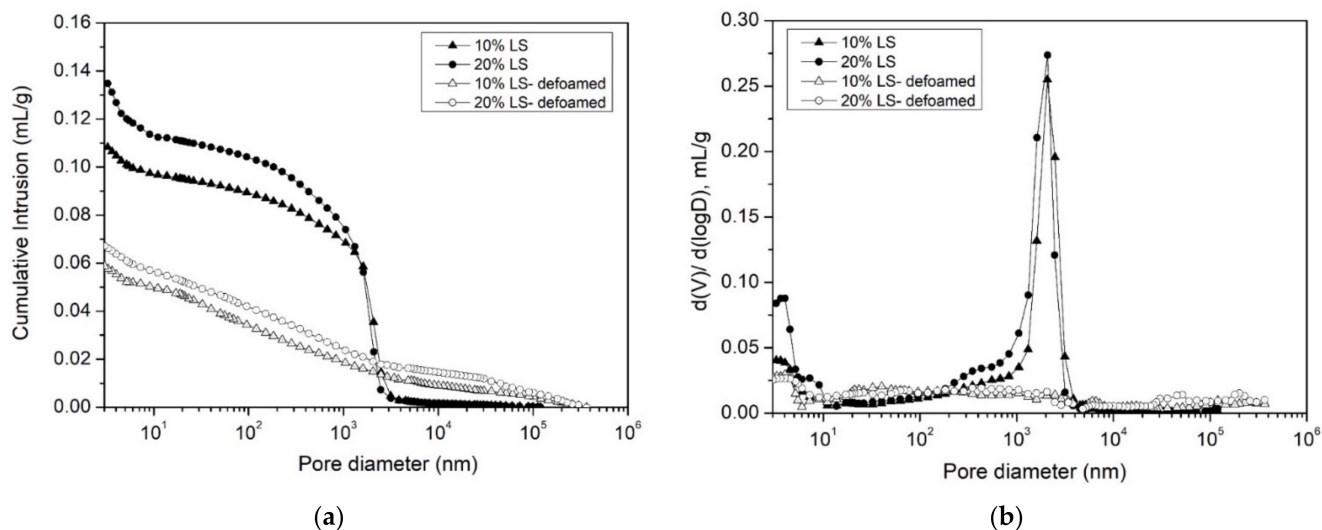


**Figure 10.** Mercury intrusion porosimetry (MIP) results on MAPC mortar samples with limestone fines (LS) at content of 10% and 20% with or without defoaming treatment by the compound use of 0.3% polyether modified silicone (PMS) defoamer and 1% Portland cement (PC): (a) Cumulative intrusion; (b) differential pore-size distribution.

In the meantime, the pore size distribution of reference samples with limestone fines (10% and 20%) suggested that the interior pores of the mortar matrix were mainly macropores larger than 1  $\mu\text{m}$  (Figure 10b). Normally the pores larger than 200 nm are considered harmful to compressive strength of cementitious matrix [37–39]. Macropores are more

likely to be the weak points for cracking under loading, which explains the decrease in compressive strength as aforementioned. These pores also provide migration channel for invasion of water or harmful ions, leading to durability degradation. After defoaming treatment, the macropores larger than 1  $\mu\text{m}$  were significantly reduced and the pore structure was modified to be finer. The MIP results were consistent with improved mechanical strength and durability properties of defoamed samples.

#### 4. Conclusions

This study has explored the feasibility of preparing MAPC mortar using manufactured limestone sand instead of quartz sand and proposed effective modification method to improve the properties of newly prepared MAPC mortar. Based on the results, the following conclusions can be drawn:

1. The limestone fines in manufactured sand caused significant blistering and expansion of MAPC mortar before setting and further resulted in decreased compressive strength and interfacial bonding strength. The blistering was inferred to be induced by generation of  $\text{CO}_2$  from the reaction between  $\text{CaCO}_3$  and ADP.
2. The polyether modified silicone (PMS) defoamer had a certain effect on breaking bubbles and reducing partial expansion caused by limestone fines. The addition of 0.3% PMS (by weight of MAPC) achieved around 50% reduction in expansion. But higher dosage of PMS caused a decrease in fluidity of MAPC mortar which weakened the defoaming effect on the contrary.
3. The compound addition of silica fume did not show enhancement on the defoaming effect on the basis of PMS defoamer.
4. The compound use of PMS defoamer and Portland cement showed significant effectiveness in disappearing and inhibiting bubbles caused by limestone fines in MAPC mortar. The strong alkalinity of Portland cement and its reactive mineral contents enable it to fast react with ADP and suppress the bubbling reaction of limestone fines ( $\text{CaCO}_3$ ). The addition of 0.3% PMS defoamer and 1% Portland cement achieved almost 90% reduction in expansion and this formula was tested to be effective for different content of limestone fines at 10% and 20%.
5. After treatment by the compound defoaming admixture, MAPC mortar containing limestone fines obtained enhanced compressive strength, interfacial bonding strength and impermeability performance including resistance to chloride ion penetration and water-tightness.
6. The MIP test results confirmed that the blistering and expansion caused by limestone fines resulted in a porous structure of MAPC mortar with high porosity and lots of macropores larger than 1  $\mu\text{m}$ . After treatment by the compound defoaming admixture, the pore structure of MAPC mortar was modified to be finer with lower porosity and much less macropores.

**Author Contributions:** Conceptualization, W.M.; methodology, W.M.; software, W.M. and C.C.; validation, W.M. and C.C.; formal analysis, W.M.; investigation, W.M. and C.C.; resources, W.M. and C.Y.; data curation, W.M. and C.C.; writing—original draft preparation, W.M.; writing—review and editing, W.M.; visualization, W.M.; supervision, X.L. and J.Q.; project administration, W.M. and X.L.; funding acquisition, X.L. and W.M. All authors have read and agreed to the published version of the manuscript.

**Funding:** This research was funded by Yunnan Province Science and Technology Projects, grant number 202004AR040017; 202001AU070069. The APC was funded by Yunnan Academy of Building Research Co., Ltd.

**Acknowledgments:** The support for this research work from Yunnan Province Science and Technology Department is gratefully acknowledged.

**Conflicts of Interest:** The authors declare no conflict of interest.

## References

1. Walling, S.A.; Provis, J.L. Magnesia-based cements: A journey of 150 Years, and cements for the future? *Chem. Rev.* **2016**, *116*, 4170–4204. [[CrossRef](#)]
2. Qian, J. 4-Magnesium phosphate cement. In *Magnesia Cements*; Shand, M.A., Al-Tabbaa, A., Qian, J., Mo, L., Jin, F., Eds.; Elsevier: Amsterdam, The Netherlands, 2020; pp. 85–170; ISBN 9780123919250. [[CrossRef](#)]
3. Yang, Q.; Zhu, B.; Wu, X. Characteristics and durability test of magnesium phosphate cement-based material for rapid repair of concrete. *Mat. Struct.* **2000**, *33*, 229–234. [[CrossRef](#)]
4. Haque, M.A.; Chen, B. Research progresses on magnesium phosphate cement: A review. *Constr. Build. Mater.* **2019**, *211*, 885–898. [[CrossRef](#)]
5. Qiao, F.; Chau, C.K.; Li, Z. Property evaluation of magnesium phosphate cement mortar as patch repair material. *Constr. Build. Mater.* **2010**, *24*, 695–700. [[CrossRef](#)]
6. Yang, N.; Shi, C.; Yang, J.; Chang, Y. Research progresses in magnesium phosphate cement-based materials. *J. Mater. Civ. Eng.* **2014**, *26*, 04014071–4014078. [[CrossRef](#)]
7. You, C.; Qian, J.; Qin, J.; Wang, H.; Wang, Q.; Ye, Z. Effect of early hydration temperature on hydration product and strength development of magnesium phosphate cement (MPC). *Cem. Concr. Res.* **2015**, *78*, 179–189. [[CrossRef](#)]
8. Qin, J.; Qian, J.; You, C.; Fan, Y.; Li, Z.; Wang, H. Bond behavior and interfacial micro characteristics of magnesium phosphate cement onto old concrete substrate. *Constr. Build. Mater.* **2018**, *167*, 166–176. [[CrossRef](#)]
9. Jia, X.; Li, J.; Wang, P.; Qian, J.; Tang, M. Preparation and mechanical properties of magnesium phosphate cement for rapid construction repair in ice and snow. *Constr. Build. Mater.* **2019**, *229*, 116927. [[CrossRef](#)]
10. Ma, C.; Wang, F.; Zhou, H.; Jiang, Z.; Ren, W.; Du, Y. Effect of early-hydration behavior on rheological properties of borax-admixed magnesium phosphate cement. *Constr. Build. Mater.* **2021**, *283*, 122701. [[CrossRef](#)]
11. Yang, Q.; Wu, X. Factors influencing properties of phosphate cement-based binder for rapid repair of concrete. *Cem. Concr. Res.* **1999**, *29*, 389–396, ISSN 0008-8846. [[CrossRef](#)]
12. Yue, L.; Bai, W.; Shi, T. A study of the bonding performance of magnesium phosphate cement on mortar and concrete. *Constr. Build. Mater.* **2017**, *142*, 459–468. [[CrossRef](#)]
13. Wang, Y.S.; Dai, J.G.; Wang, L.; Tsang, D.C.W.; Poon, C.S. Influence of lead on stabilization/solidification by ordinary Portland cement and magnesium phosphate cement. *Chemosphere* **2018**, *190*, 90–96. [[CrossRef](#)] [[PubMed](#)]
14. Xiao, J.; Xu, Z.; Murong, Y.; Wang, L.; Lei, B.; Chu, L.; Jiang, H.; Qu, W. Effect of Chemical Composition of Fine Aggregate on the Frictional Behavior of Concrete–Soil Interface under Sulfuric Acid Environment. *Fractal Fract.* **2022**, *6*, 22. [[CrossRef](#)]
15. Lei, W.; Luo, R.Y.; Zhang, W. Effects of fineness and content of phosphorus slag on cement hydration, permeability, pore structure and fractal dimension of concrete. *Fractals* **2021**, *29*, 2140004. [[CrossRef](#)]
16. Wang, L.; Lu, X.; Liu, L.; Xiao, J.; Zhang, G.; Guo, F.; Li, L. Influence of MgO on the hydration and shrinkage behavior of low heat Portland cement-based materials via pore structural and fractal analysis. *Fractal Fract.* **2022**, *6*, 40. [[CrossRef](#)]
17. Wang, D.; Shi, C.; Farzadnia, N.; Shi, Z.; Jia, H. A review on effects of limestone powder on the properties of concrete. *Constr. Build. Mater.* **2018**, *192*, 153–166. [[CrossRef](#)]
18. Liu, S.; Yan, P. Effect of limestone powder on microstructure of concrete. *J. Wuhan Univ. Technol. Mat. Sci. Edit.* **2010**, *25*, 328–331. [[CrossRef](#)]
19. *ASTMC939-10*; Standard Test Method for Flow of Grout for Preplaced-Aggregate Concrete (Flow Cone Method). ASTM International: West Conshohocken, PA, USA, 2010. Available online: <https://standards.globalspec.com/std/3840648/ASTM%20C939-10>(accessed on 26 January 2022).
20. *ASTMC187-10*; Standard Test Method for Normal Consistency of Hydraulic Cement. ASTM International: West Conshohocken, PA, USA, 2010. Available online: <https://standards.globalspec.com/std/3839853/astm-c187-10>(accessed on 26 January 2022).
21. *JTG 3420-2020 (T 0518-2020)*; Testing Methods of Cement and Concrete for Highway Engineering: Testing Method for Free Bleeding Rate and Free Expansion Rate of Cement Slurry. Ministry of Transport of the People’s Republic of China: Beijing, China, 2020.
22. *ASTMC596-18*; Standard Test Method for Drying Shrinkage of Mortar Containing Hydraulic Cement. ASTM International: West Conshohocken, PA, USA, 2018. Available online: <https://standards.globalspec.com/std/13162334/astm-c596-18>(accessed on 26 January 2022).
23. *ISO 679:2009*; Cement—Test Methods—Determination of Strength. ISO/TC 74: Geneva, Switzerland, 2009. Available online: <https://www.iso.org/standard/45568.html>(accessed on 26 January 2022).
24. *GB/T 50081-2002*; Standard for Test Method of Mechanical Properties on Ordinary Concrete. Ministry of Construction of the People’s Republic of China: Beijing, China, 2002.
25. *JGJ/T 70-2009*; Standard for Test Method of Performance on Building Mortar. Ministry of Construction of the People’s Republic of China: Beijing, China, 2009.
26. *ASTMC 1202-2012*; Standard Test Method for Electrical Indication of Concrete’s Ability to Resist Chloride Ion Penetration. ASTM International: West Conshohocken, PA, USA, 2012. Available online: <https://salmanco.com/wp-content/uploads/2017/06/ASTM-c-1202.pdf>(accessed on 26 January 2022).
27. Chong, L.; Shi, C.; Yang, J.; Jia, H. Effect of limestone powder on the water stability of magnesium phosphate cement-based materials. *Constr. Build. Mater.* **2017**, *148*, 590–598. [[CrossRef](#)]

28. Yang, Q.; Zhu, B.; Zhang, S.; Wu, X. Properties and applications of magnesia–phosphate cement mortar for rapid repair of concrete. *Cem. Concr. Res.* **2000**, *30*, 1807–1813. [[CrossRef](#)]
29. Xing, J.; Bi, Y.; Li, X.; Xiong, L. The Influence of Different Anti-foaming Agent on Concrete. In Proceedings of the 4th International Conference on Mechanical Materials and Manufacturing Engineering (MMME 2016), Wuhan, China, 15–16 October 2016.
30. Zheng, D.; Ji, T.; Wang, C.Q.; Sun, C.J.; Lin, X.J.; Hossain, K.M.A. Effect of the combination of fly ash and silica fume on water resistance of Magnesium–Potassium Phosphate Cement. *Constr. Build. Mater.* **2016**, *106*, 415–421. [[CrossRef](#)]
31. Tong, W. Study on the Properties of Mineral Admixture and Portland Cement Modified Magnesium Phosphate Cement. Ph.D. Thesis, Xi’an University of Architecture and Technology, Xi’an, China, 2016. Available online: <https://kns.cnki.net/kcms/detail/detail.aspx?dbcode=CMFD&dbname=CMFD201701&filename=1016739902.nh&uniplatform=NZKPT&v=jBM3Qj%25mmd2F9zandtWT5jc8UC1eNB%25mmd2Bxj9OHOSDhjGf%25mmd2FYLz2%25mmd2BhkDbxZHLEXDxl6> (accessed on 8 January 2022). (In Chinese)
32. Xu, X.; Lin, X.; Pan, X. Influence of silica fume on the setting time and mechanical properties of a new magnesium phosphate cement. *Constr. Build. Mater.* **2020**, *235*, 117544. [[CrossRef](#)]
33. Qin, Z.; Ma, C.; Zheng, Z. Effects of metakaolin on properties and microstructure of magnesium phosphate cement. *Constr. Build. Mater.* **2020**, *234*, 117353. [[CrossRef](#)]
34. Liu, Y.; Chen, B.; Dong, B.; Wang, Y.; Xing, F. Influence mechanisms of fly ash in magnesium ammonium phosphate cement. *Constr. Build. Materials.* **2022**, *314*, 125581. [[CrossRef](#)]
35. Jiang, Z.; Qian, C.; Chen, Q. Experimental investigation on the volume stability of magnesium phosphate cement with different types of mineral admixtures. *Constr. Build. Mater.* **2017**, *157*, 10–17. [[CrossRef](#)]
36. Wang, L.; Song, X.; Yang, H.; Wang, L.; Tang, S.; Wu, B.; Mao, W. Pore structural and fractal analysis of the effects of MgO reactivity and dosage on permeability and F–T resistance of concrete. *Fractal Fract.* **2022**, *6*, 113. [[CrossRef](#)]
37. Lian, H.; Shi, H. Clarification of a Hypothesis on Centropiasm of Cement-based Composite’ Proposed by Wu Zhongwei. *J. Chin. Ceram. Soc.* **2020**, *48*, 777–786. [[CrossRef](#)]
38. Huang, J.; Li, W.; Huang, D. Fractal analysis on pore structure and hydration of magnesium oxysulfate cements by first principle, thermodynamic and microstructure-based methods. *Fractal Fract.* **2021**, *5*, 164. [[CrossRef](#)]
39. Lei, W.; Jin, M.; Guo, F.; Wang, Y.; Tang, S. Pore structural and fractal analysis of the influence of fly ash and silica fume on the mechanical property and abrasion resistance of concrete. *Fractals* **2021**, *29*, 2140003. [[CrossRef](#)]